Journal of Physiology (1991), **435**, *pp.* 207–228
With 9 figures
Printed in Great Britain

THE MEDULLARY PROJECTIONS OF AFFERENT BRONCHOPULMONARY C FIBRES IN THE CAT AS SHOWN BY ANTIDROMIC MAPPING

BY L. KUBIN, H. KIMURA AND R. O. DAVIES

From the Department of Animal Biology, School of Veterinary Medicine and the Pulmonary Section, School of Medicine, University of Pennsylvania, Philadelphia, PA 19104, USA

(*Received 17 July 1990*)

SUMMARY

1. The activity of eighty-seven bronchopulmonary vagal afferent neurones with unmyelinated axons (C fibres) was recorded extracellularly in the nodose ganglia of decerebrate, paralysed and artificially ventilated cats. On the basis of their response latencies following the right atrial injection of capsaicin or phenyldiguanide, the cells were classified as having their receptor endings within the reach of pulmonary (latency less than 3·5 s) or bronchial (latency above 3·5 s) circulation.

2. Pulmonary and bronchial receptor cells differed only slightly in their response characteristics (firing rate, burst duration) and the conduction velocity of their peripheral axons. Bronchial C fibres represented about 70% of the population studied.

3. The medullary distributions of the central branches of six pulmonary and six bronchial C fibres were determined by means of the antidromic mapping technique. The two receptor subtypes did not differ in their central projection patterns.

4. Rostral to the obex, the central branches of the bronchopulmonary C fibres were localized within the medial portions of the nucleus tractus solitarii (NTS) and area postrema, and were most densely distributed along the borders of the parvicellular subnucleus of the NTS. Caudal to the obex, the most dense branching was found in the dorsal portion of the commissural subnucleus. Projections to the contralateral NTS were found, but these were of a much lower density.

5. The central distribution of bronchopulmonary C fibres is compared to the projection patterns of vagal and glossopharyngeal afferents of other modalities that are involved in respiratory and cardiovascular control. This is discussed in relation to the concept of a modality-specific organization of the NTS.

INTRODUCTION

Non-myelinated afferent neurones from the lung parenchyma and intrapulmonary airways (bronchopulmonary C fibres) constitute about 75–90% of the sensory fibres in the pulmonary branches of the vagus nerve (Agostoni, Chinnock, Daly & Murray, 1957; Mei, Condamin & Boyer, 1980; Jammes, Fornaris, Mei & Barrat, 1982). Most C fibre endings in the lower respiratory tract are polymodal receptors that respond

to a variety of chemical, thermal and mechanical stimuli, such as phenyldiguanide, capsaicin, autacoids, CO_2, lung inflation and hyperdeflation, pulmonary oedema and embolism (see Paintal, 1973; Coleridge & Coleridge, 1984 for reviews). Mass chemical stimulation of C fibres causes apnoea followed by rapid, shallow breathing, bradycardia and hypotension. However, even the low, tonic activity of C fibres may play an important role in the reflex control of ventilatory volume and timing, airway smooth muscle tone, heart rate and vascular smooth muscle tone in both normal and pathological situations (see Paintal, 1973; Coleridge & Coleridge, 1984 for reviews). The central neural pathways through which these reflex effects are produced are unknown.

Previous neuroanatomical investigations in the cat (Kerr, 1962; Cottle, 1964; Kalia & Mesulam, 1980*a*) have shown that vagal afferent fibres terminate principally in the nucleus tractus solitarii (NTS). More specifically, when the neuroanatomic tracer horseradish peroxidase (HRP) was injected directly into the lung parenchyma, the receptors or fibres that took up the protein had their heaviest projections to the ipsilateral ventrolateral, dorsolateral and commissural subnuclei of the NTS (Kalia & Mesulam, 1980*b*). In contrast, after injections of the tracer into the main bronchus, projections to the ventrolateral, intermediate and interstitial subnuclei were most pronounced. In both cases, there were also substantial projections to other subnuclei bilaterally as well as to the area postrema. Recently, Torrealba & Calderón (1990), using the Wallerian degeneration technique, demonstrated that unmyelinated vagal afferent fibres project mainly to the medial, commissural, dorsal and gelatinosus subnuclei, while thicker afferents occupy predominantly the lateral and ventrolateral regions of the NTS. However, such anatomic studies do not allow one to distinguish the projection patterns to the various subnuclei of fibres of different sensory modalities. We have begun our study of the bronchopulmonary C fibre reflex pathway by determining the medullary sites of the central projections of individual C fibre neurones. For that, we have used the antidromic mapping technique (see Lipski, 1981) to determine the course of the central pathways and localize the regions of termination within the NTS of single, functionally identified C fibre afferents whose activity was recorded in the nodose ganglion. This same protocol has proved successful for the mapping of slowly adapting pulmonary stretch receptor neurones (Donoghue, Garcia, Jordan & Spyer, 1982), carotid body chemoreceptor afferents with non-myelinated axons (Donoghue, Felder, Jordan & Spyer, 1984) and pulmonary rapidly adapting receptor neurones (Davies & Kubin, 1986).

Preliminary reports have been published elsewhere (Kubin & Davies, 1987, 1989).

METHODS

Animal preparation

The results reported are from experiments on nineteen cats of either sex, weighing 1·9–4·1 kg. The cats were pre-anaesthetized with ketamine (70 mg, I.M.), and given dexamethasone (2 mg, I.M.) to minimize brain oedema, and atropine (2 mg, I.M.) to prevent airway secretions. Following intubation, the animals were anaesthetized with halothane and decerebrated (Kirsten & St. John, 1978). Anaesthesia was then discontinued.

The animal preparation and recording procedures were similar to those described in our previous study of the central projections of pulmonary rapidly adapting receptors (Davies & Kubin, 1986). Catheters were placed in the femoral artery and vein for blood pressure monitoring and drug

administration, respectively. Another catheter was placed in the left jugular vein and advanced about 11 cm down-stream to the right atrium. It was used for injection of substances that excite bronchopulmonary C fibres. The C5 branch of the left phrenic nerve was exposed, cut distally and desheathed for whole-nerve recording. The right nodose ganglion was exposed by a lateral approach and dissected free from the surrounding tissue. The animal was then connected to a respirator, the thorax opened through the second intercostal space, and the right vagus nerve dissected in continuity on the intrathoracic trachea. A cuff electrode was implanted for subsequent stimulation of the nerve and the thorax closed. The cervical vagus nerve was also prepared for stimulation low in the neck. The cat was then placed in a stereotaxic frame with the head ventroflexed at 45 deg and vertebral clamps at T2 and L2. The caudal medulla was exposed for electrical microstimulation within the region of the NTS. The animals were paralysed with gallamine triethiodide (Flaxedil, Davis & Geck; 10 mg, I.V., followed by a continuous infusion of 5 mg kg^{-1} h^{-1}) and artificially ventilated. A pneumothorax was made and an expiratory load of 1–2 cmH_2O imposed.

The tracheal CO_2 concentration was monitored (Puritan-Bennett, Datex CO_2 Monitor) and maintained constant at a concentration between 3·5–5·0%. In some experiments, oxygen was added to the inspired air. Systemic arterial blood pressure, tracheal pressure and airflow were continuously monitored. When necessary, methoxamine hydrochloride (Vasoxyl, Burroughs Wellcome) was infused to maintain the mean blood pressure above 80 mmHg. In some experiments, naloxone was also infused at a rate of 0·5 mg h^{-1} as we found it to be helpful in preventing hypotension and antidromic conduction failures in the studied fibres throughout the prolonged electrical stimulation within the medulla. The rectal temperature was maintained at 37·5–38·5 °C by a servo-controlled heating pad. A thermistor probe and a resistor heated by direct current were placed in the paraffin pool surrounding the vagus nerve and the nodose ganglion, and were used to monitor the temperature of the pool and maintain it at 33–35 °C.

Neural recording and stimulation

Single-cell activity was recorded extracellularly in the nodose ganglion with aluminosilicate glass microelectrodes filled with 3 M-NaCl. The tips were mechanically broken to give a diameter of 0·8–1·8 μm (resistance, 1·4–2·5 MΩ). The nodose ganglion was supported on a silver plate, which also served as a reference electrode. The microelectrodes were advanced by a stepping motor, hydraulic microdrive (Haer). Single-cell action potentials were amplified (Grass P511) and fed to a window discriminator to provide standard pulses. The pulses were counted with a microprocessor-based moving average counter (CWE, Inc., Model DMA-931; window width 200 ms, advanced in time every 1 ms).

Medullary microstimulation was made with monopolar, gold and platinum plated micro-electrodes (NeuroLog type 02) having initial resistance of 0·1–0·2 MΩ. The electrode penetrations were made with a stepping motor microdrive (Transvertex). Electrical stimulations were done using a Grass stimulator (Model S88) and constant current isolation unit (PSIU6). Monophasic, rectangular current pulses having a duration of 500 μs and an amplitude not exceeding 500 μA were used.

The vagus nerve was stimulated electrically with single pulses of 500 μs duration and a strength corresponding to 3–5 times the threshold for evoking a C fibre wave as recorded in the nodose ganglion. The distance from the electrode to the ganglion was 42–52 mm for the cervical electrode and 80–120 mm for the thoracic electrode.

Phrenic nerve activity was recorded with a bipolar electrode, amplified (Grass P511), rectified and processed by a low pass, third order Paynter filter with a time constant of 100 ms to compute the moving average of the neural activity.

Neural activities, as well as tracheal pressure, airflow and stimulus markers, were recorded on a chart recorder (Gould, TA2000) and an eight track FM tape recorder (Hewlett-Packard, 3968A).

Experimental protocol

Because most nodose ganglion neurones with non-myelinated axons have very low spontaneous firing rates (Coleridge & Coleridge, 1984), the ganglion was explored during continuous, 1 Hz, stimulation of the vagus nerve. We tested each cell isolated during vagal stimulation that had a conduction velocity less than 2·5 m s^{-1} for its response to a bolus injection of 60 μg capsaicin (0·2 ml) and/or 160 μg phenyldiguanide solution (0·4 ml) into the right atrium. Cells excited by

such an injection with a latency shorter than 3·5 s were regarded as having their receptor endings within the reach of pulmonary circulation; those responding with longer latencies were classified as bronchial receptors (Coleridge & Coleridge, 1984).

The search for the central endings of pulmonary or bronchial C fibres identified in this manner usually began with microstimulation in the proximity of the ipsilateral solitary tract, about 2 mm rostral to the obex. This allowed us to verify that the central axon of the cell selected for mapping reached that medullary region. Subsequent penetrations were placed in the ipsilateral NTS caudal to the obex. If central branches of the cell were found in this latter region, the stimulating electrode was moved to the contralateral NTS, about 1 mm rostral to the obex. From that point, we started a systematic mapping series, changing the position of subsequent penetrations by 0·2–0·5 mm medio-laterally or rostro-caudally. In each penetration, the electrode was advanced in 100 or 50 μm steps. In each track, the latencies of the antidromic responses recorded from the cell in the nodose ganglion were measured, together with the depth of stimulation. Sites at which responses with distinct latencies could be evoked by varying the stimulus intensity were regarded as containing several branches (one for each latency) of the cell under study (see Davies & Kubin, 1986). The collision test (see Lipski, 1981) was used several times during the mapping to verify that the responses originated from branches of the same cell.

At the end of the experiment, a single medullary site containing branches of the cell studied was marked by passing a 20 μA current for 30 s (electrode tip negative). The cat was then perfused with 10% formalin in saline through the femoral artery. The medulla was removed and, subsequently, serial, transverse sections, 50 μm thick, were cut on a freezing microtome, stained with Neutral Red and mounted for examination.

Reconstruction of the central projection

The location of each penetration was determined on the basis of its co-ordinates with respect to the obex, the location of the microlesion placed at the end of mapping, and inspection of the serial sections of the medulla. At the high currents that we had to use in this study to activate C fibre central endings from a distance of at least 0·2 mm (see Results), each electrode penetration left a noticeable track in the tissue. Thus, the actual position of most penetrations with respect to NTS subnuclei could be determined despite the limited accuracy (± 50 μm) of the stereotaxic co-ordinate readings, the occurrence of tissue displacements in regions of dense tracking and tissue shrinkage during histological processing. The position of each penetration was then superimposed on a corresponding camera lucida drawing of a transverse section. The location of each track was also plotted on a map showing a dorsal view of the medial and lateral borders of the NTS; this map was drawn for each experiment from measurements taken from the serial sections.

For each penetration, depth–threshold curves were plotted for each response characterized by a distinct latency. The curves were analysed to yield an estimate of effective current spread for individual central branches and thus to determine the distance between the stimulating electrode tip and the stimulated fibre. The analysis was based on interpolation of individual curves by a second order polynomial, $y = Ax^2 + Bx + C$, and the 'A' coefficient was used to characterize the steepness of individual curves (see Davies & Kubin, 1986 for a full description of the analysis). For those sets of penetrations for which the same central branch of the cell under study could have been stimulated at different sites along its course, distance–latency plots were constructed to verify such a possibility (see Davies & Kubin, 1986). The final drawings of dorsal views of the NTS showing the distribution of C fibre endings represent semi-schematic reconstructions of the supposed course of the fibres (as explained in the Results), while the drawings of individual coronal cross-sections show the actual distribution of the minimum threshold points found in penetrations made within 0·25 mm, rostro-caudal, of the level of the cross-section.

The variability of mean values was characterized throughout this report by a standard deviation (S.D.) and a two-tailed Student's t test was used to assess the differences between the means.

RESULTS

General characteristics of the cells studied

In nineteen cats, we have tested about 700 nodose ganglion cells with peripheral axonal conduction velocities equal to, or less than, 2·5 m s^{-1} for their responses to capsaicin or phenyldiguanide injected into the right atrium. Eighty-seven cells

(12%) were excited with latencies ranging from 0·5 to 15 s (Fig.1). Of those, twenty-three were recorded with a satisfactory signal-to-noise ratio so that we attempted to search for their central axons by means of electrical stimulation within the medulla. The central projections of eleven cells could not be mapped, either because they could

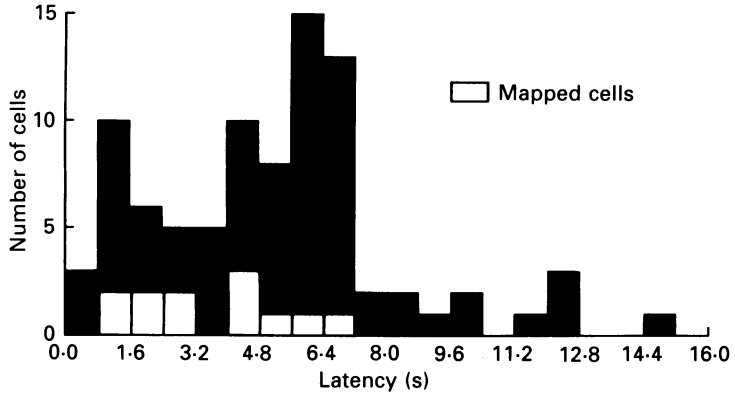

Fig. 1. Distribution of response latencies of 87 bronchopulmonary C fibres to the injection of capsaicin or phenyldiguanide into the right atrium. The latency was measured from the onset of a rapid injection of 0·2–0·4 ml of the drug to the first action potential in the evoked burst of spikes. Note that the histogram shows two peaks, one around a latency of 1·2 s and another within the 4·0–7·2 s range. C fibres whose central projections were mapped in this study are shown by white bars. Six of these responded with a latency within the early peak (pulmonary receptors) and six with a latency covered by the second peak of the histogram (bronchial receptors).

not be antidromically excited from the solitary tract region (possibly because their central axons were damaged by earlier penetrations in the ganglion (nine cells)) or were lost very early during the mapping (two cells). The distributions of central branches of the remaining twelve cells, one cell per experiment, were successfully mapped, at least in part, and the rest of this report is based on the data obtained from this latter group.

Six of the mapped cells were excited by capsaicin and/or phenyldiguanide with the shortest latencies ranging from 1·0 to 3·2 s (mean, $2·1 \pm 0·9$ s) and were classified as pulmonary C fibre neurones. The other six cells displayed latencies ranging from 4·1 to 6·9 s (mean, $5·2 \pm 1·0$ s) and were classified as bronchial C fibre neurones. Figure 2*A* and *B* shows examples of responses to capsaicin of a pulmonary and a bronchial receptor cell, respectively. Figure 1 shows a histogram of response latencies of all the cells that we found that responded to capsaicin, with those that were successfully mapped distinguished by white bars. The histogram shows a weak bimodal distribution; one peak within the latency range of 0–3·2 s and the other within the 3·2–7·2 s range. This corresponds well to the classification of bronchopulmonary C fibres obtained by sampling of single vagal afferent fibres (cf. Coleridge & Coleridge, 1984). Seventy-two percent of the eighty-seven receptors that responded did so with a latency greater than 3·2 s.

The duration of the burst of action potentials produced by capsaicin and the mean firing rate within the burst in the six pulmonary cells were $3·9 \pm 2·0$ s and $8·6 \pm 4·3$ impulses s^{-1}, respectively. The corresponding measures for the six bronchial cells

were 5·8 ± 1·7 s and 4·4 ± 2·5 impulses s^{-1} ($P < 0·1$ for both comparisons between pulmonary and bronchial cells). One pulmonary and three bronchial cells showed irregular spontaneous firing at rates of 0·17–1·0 impulses s^{-1} while the remaining mapped cells were not spontaneously active. For one pulmonary cell, satisfactory

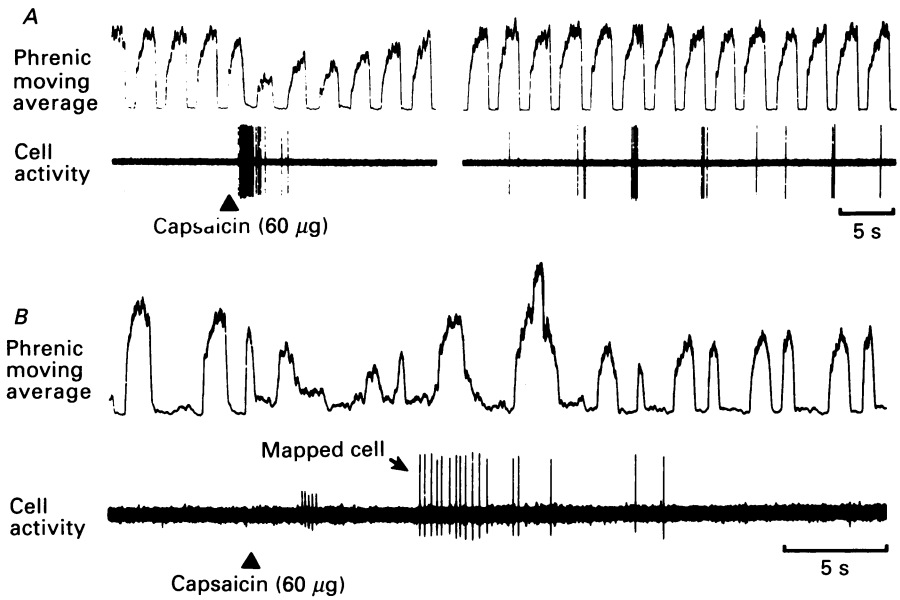

Fig. 2. Two examples of responses of bronchopulmonary C fibres to capsaicin. *A*, a pulmonary C fibre. The left panel shows that latency of the response is less than 1 s and there is a concomitant inhibition of the phrenic nerve activity. The right panel shows that the receptor endings of this cell responded to mechanical probing within the middle lung lobe. *B*, simultaneously recorded responses to capsaicin of a pulmonary (small spikes) and a bronchial (large spikes) C fibre.

recording of its activity was maintained until the end of the experiment. That allowed us to open the thorax widely and localize by mechanical probing the receptive field of this cell within the middle lobe of the lung (Fig. 2*A*, right panel).

The mean conduction velocity of the peripheral axons of the six pulmonary cells was 1·1 ± 0·4 m s^{-1} (range, 0·73–1·87 m s^{-1}), and for the six bronchial cells 0·85 ± 0·05 m s^{-1} (range, 0·79–0·91 m s^{-1}) ($P < 0·15$).

Antidromic excitation of bronchopulmonary C fibres from the NTS region

At the beginning of each mapping session, the medullary electrode was placed close to the ipsilateral solitary tract, rostral to the obex, in order to make sure that the cell to be studied projected at least to that medullary region. The latency of the antidromic response evoked from these sites was, as a rule, the shortest of all those subsequently obtained for each cell. The six pulmonary cells were excited with an average latency of 40 ± 7 ms (range, 29–48 ms), while the six bronchial cells had a latency of 50 ± 13 ms (range, 38–75 ms). Use of an average length of 25 mm (or 30 mm for larger animals) for the distance between the solitary tract and the nodose

ganglion (Donoghue *et al.* 1982) to calculate the conduction velocity in the proximal portions of the central axons gave average values of $0{\cdot}64 \pm 0{\cdot}1$ m s^{-1} for the pulmonary fibres and $0{\cdot}54 \pm 0{\cdot}1$ m s^{-1} for the bronchial fibres ($P < 0{\cdot}1$).

After locating the central axon of the cell close to the solitary tract, we started a systematic tracking in the NTS. Nine to fifty-seven penetrations were made in

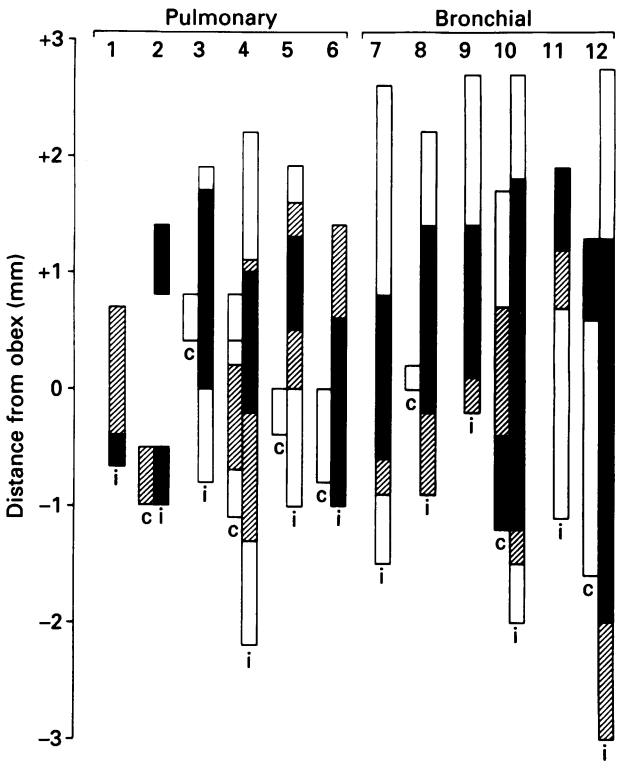

Fig. 3. Rostro-caudal distribution of stimulation sites within the NTS in individual mapping sessions. The vertical bars show the total longitudinal extent of mapping for all six pulmonary (numbers 1–6) and all six bronchial (numbers 7–12) C fibres at different levels relative to the obex: i, ipsilateral; c, contralateral. The bars are hatched at those levels where two branches were detected in some penetrations and filled at those levels where three or more branches were detected. Both fibre types showed heavy branching at the same rostro-caudal levels.

individual experiments (average, 32) depending on the extent of the cell's arborization, and the duration of maintaining a stable recording of the activity of the cell with a satisfactory signal to noise ratio. The latency of the antidromically evoked response increased as penetrations were placed further caudad. The longest latencies of antidromic responses obtained from the caudal NTS were 18 ± 8 ms (range, 10–32 ms) longer than those obtained from the rostral-most points within the ipsilateral solitary tract. There was no orderly relationship between this maximal latency difference and the conduction velocity of the proximal part of central axon.

In many penetrations, responses with different latencies were obtained by

stimulating at slightly different depths. In addition, changing the stimulus intensity at a single site often resulted in a sudden change of the latency. These effects were taken to indicate the presence of several distinct branches of the studied cell within the stimulated region (cf. Lipski, 1981; Davies & Kubin, 1986). Figure 3 shows, for each cell, the rostro-caudal extent of the penetrations placed within the NTS region. The black portions of the bars show those levels where three or more branches were detected in individual penetrations, while the open segments indicate those levels where either no response was obtained or just the main axon was stimulated with no evidence of branching. With eight cells, we searched for branching in the contralateral NTS (bars marked by 'c'). For five of these cells, some degree of branching, or at least the main axon (cell 3) was detected contralaterally. In five of the twelve studies, we used closely spaced penetrations within the ipsilateral and/or contralateral commissural region and were able to exclude the possibility that some axonal branches crossed to the contralateral NTS. For the two remaining cells (numbers 1 and 9), such a possibility could not be completely ruled out.

The course of the neurone's main axon was determined for each cell on the basis of the response latencies and corresponding threshold values, and the location of the penetrations as determined from the serial sections of the brains. To do that, we performed a distance–latency analysis to see if the latency of the antidromic response increased steadily along the supposed course of the axon. Figure 4*A* shows the distribution of penetrations from one experiment superimposed on a dorsal view of the NTS. The numbers shown next to each track give the shortest antidromic latency found in that penetration. One may notice that penetrations located in or close to the solitary tract yielded responses with the shortest latencies at any given rostro-caudal level, which suggests that the cell's main axon coursed along the tract. Figure 4*B* shows three distance–latency plots and linear regression lines drawn separately for those points shown in Fig. 4*A* that were distributed: along the rostral and intermediate portion of the solitary tract ipsilaterally; further caudally and medially within the commissural region; and within the medial portion of the contralateral NTS, respectively. The slopes of the regression lines fitted to the ipsilaterally located points gave similar conduction velocities, 0·44 and 0·52 m s^{-1}. The conduction velocity determined for the contralaterally located points was substantially lower (0·15 m s^{-1}). The estimated conduction velocity for the proximal portion of this cell's axon, from the nodose ganglion to the medulla (see above), was 0·66 m s^{-1}, only slightly higher than that obtained by the distance–latency analysis of the data from the ipsilateral solitary tract. In some penetrations, responses with other, longer, latencies were also evoked at slightly different depths and/or thresholds. Such tracks are marked in Fig. 4*A* by circled symbols. It may be seen that regions of branching occupied only a fraction of the explored area.

For all six pulmonary fibres, the average conduction velocity in the solitary tract, as determined by the distance–latency analysis, was $0{\cdot}64 \pm 0{\cdot}2$ m s^{-1}. The conduction velocity in the solitary tract for five bronchial fibres was slightly lower, $0{\cdot}46 \pm 0{\cdot}06$ m s^{-1} ($P < 0{\cdot}1$). (We had insufficient data to analyse the conduction velocity for one bronchial C fibre.) These conduction velocities were similar to those obtained for the portions of central axons located between the rostral solitary tract and the nodose ganglion (see above). Thus, we did not observe any substantial

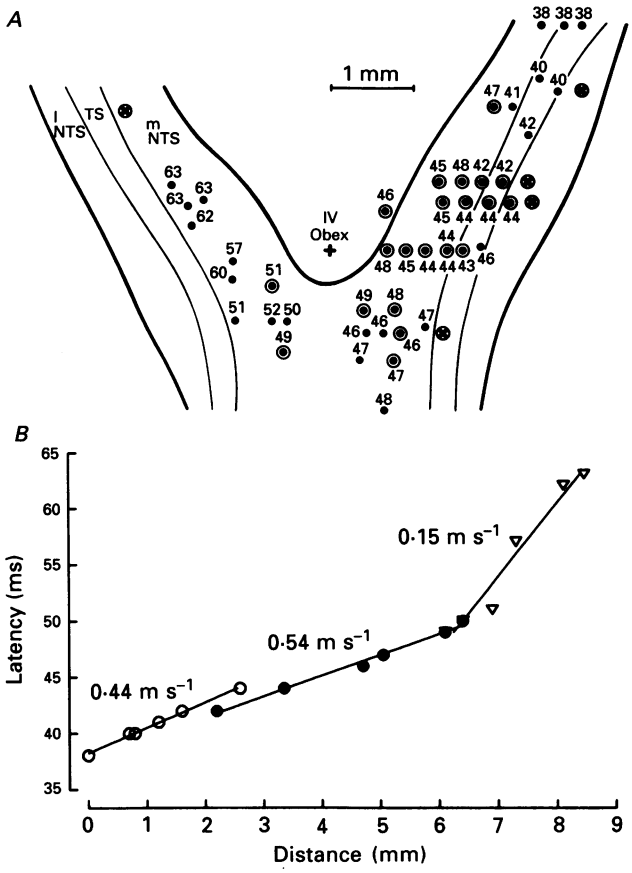

Fig. 4. *A*, distribution of penetrations in one mapping session. *B*, distance–latency plots for three portions of the main axon of the mapped cell. In *A* the locations of all the penetrations are superimposed on a dorsal view of the NTS. Medial (m) and lateral (l) portions of the nucleus on both sides are separated by the solitary tract (TS). Crossed circles (⊗) indicate penetrations from which no antidromic response was obtained. Dots (•) correspond to penetrations in which only one branch was detected and the adjacent numbers give the corresponding antidromic latency (in milliseconds). Circled dots (◉) show penetrations in which several branches of the mapped cell were stimulated; the numbers give the shortest antidromic latency only. Note that at each rostro-caudal level the shortest latencies were obtained from the region of the solitary tract and that branching was concentrated in the medial portion of the nucleus bilaterally. In *B* the latency of the antidromic response was plotted against the distance measured along the solitary tract from the most rostral penetration on the side ipsilateral to the cell body in the nodose ganglion. Separate regression lines were fitted to the points located rostral to the obex ipsilaterally, caudal and medial within the ipsilateral commissural nucleus, and within the medial portion of the contralateral NTS, respectively. The slopes of these curves give an estimate of the conduction velocities for the corresponding portions of the studied fibre. The data are for bronchial receptor cell 10 of Fig. 3.

decrease of the conduction velocity along the intramedullary course of the main axons of the C fibres, except in the presumed regions of central terminations. Moreover, our ability to fit reasonable regression lines to points distributed along the

ipsilateral solitary tract indicates that the cells' main axons assumed a relatively straight course along the tract. The mean ratio of the conduction velocities measured along the ipsilateral solitary tract to the conduction velocities of the cells' peripheral axons (distal to the nodose ganglion) was $0{\cdot}6 \pm 0{\cdot}2$ for the pulmonary and $0{\cdot}5 \pm 0{\cdot}1$ for the bronchial receptor cells. This is a smaller conduction velocity decrease than that measured in vagal afferent fibres having myelinated axons (cf. Berger & Averill, 1983; Davies & Kubin, 1986).

Spatial accuracy of the mapping

In the present study, we had to use relatively strong stimuli to be able to excite many medullary branches of the studied fibres (up to 500 μA; 0·5 ms). In our previous paper (Davies & Kubin, 1986), we have shown that interpolation of the depth–threshold curves with a parabolic equation provides a suitable means to estimate the effective current spread for individual fibres and that the steepness of these curves is inversely proportional to the conduction velocity of the stimulated branch. In this study, we have performed such analyses on a group of fifty depth–threshold curves that consisted of at least five points at different depths, displayed a smooth parabolic shape indicative of a smooth penetration of the electrode throughout the track, and had a minimum threshold of less than 70 μA. The 'A' coefficients of the second order polynomial (see Methods) were used to characterize the steepness of the curves. For example, the threshold for the curve shown in Fig. 5A, obtained by stimulation of the main axon of one of the bronchial fibres at a site close to the solitary tract rostral to the obex, increased to about 500 μA when the electrode was moved up or down from the minimum threshold point by 0·3 mm. Thus, even at a stimulus intensity of 500 μA, the tip of the stimulating electrode was located relatively close to the fibre, compared to the overall dimensions of the NTS in the cat. The 'A' coefficient for this curve was 5043 μA mm^{-2}. All but one curve analysed had 'A' coefficients higher than 4500 μA mm^{-2}.

To assess whether the conduction velocity decreased in the presumed branching regions, we divided the selected curves into four groups on the basis of the NTS region from which they were obtained. This is shown schematically in Fig. 5B (group I, ipsilateral solitary tract at levels located more than 1 mm rostral to the obex; group II, ipsilateral solitary tract from 1 mm rostral to the obex caudad; group III, the most medial portion of the ipsilateral NTS complex; group IV, contralateral NTS). Figure 5C shows the average 'A' coefficients for the four specified regions. The average values were higher than 6500 μA mm^{-2} for all regions, with a tendency for the curves obtained from regions other than the solitary tract (regions of possible branching and terminations) to display higher coefficients (over 9000 μA mm^{-2} for group III). This increase in the steepness of the depth–threshold curves indicates a decrease of fibre diameter and conduction velocity (cf. Lipski, 1981; Davies & Kubin, 1986). It may be also noticed that the variability (characterized by the S.D. of the average) of 'A' coefficients is larger for groups III and IV than for groups I and II, which probably reflects the larger variability of fibre diameters in the former two regions. The steepest depth–threshold curves obtained from regions III and IV had 'A' coefficients larger than 20000 μA mm^{-2}.

On the basis of the depth–threshold curve analysis, we concluded that the effective current spread, as characterized by 'A' coefficients, could be assumed to exceed

6000 μA mm^{-2} for a majority of the C fibre branches (other than the main axons). This meant that a current of 50 μA could excite these fibres from a distance not greater than 91 μm and the effective spread of a 250 μA stimulus was not larger than 204 μm. Thus, in our study, we distinguished between branches that were stimulated

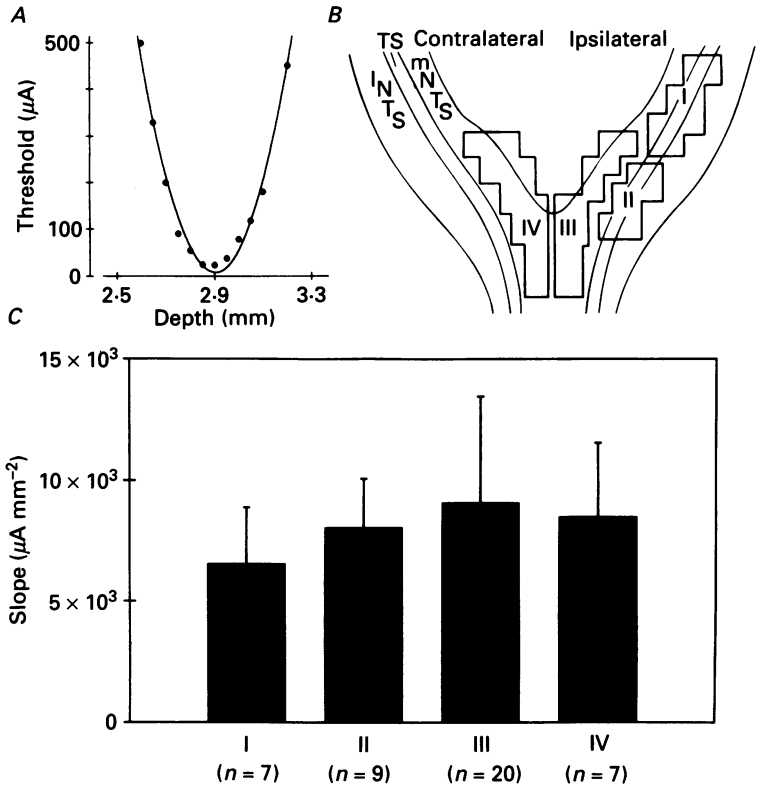

Fig. 5. Estimation of the effective current spread by monopolar stimulation of C fibres within the NTS. *A*, a typical example of a depth–threshold curve obtained by stimulation of the main axon of a C fibre near the solitary tract rostral to the obex. The steepness of the curve was characterized by the '*A*' coefficient of the second-order polynomial fitted to the experimental points ('*A*' = 5043 μA mm^{-2}, latency 42 ms). Note that moving the electrode up or down from the minimum threshold point by 0·3 mm resulted in an increase of the threshold current from almost zero to 500 μA. *B*, the four regions of the NTS from which depth threshold curves were selected to evaluate the variability of their steepness ('*A*' coefficient) are shown schematically over a dorsal view of the NTS. The regions were chosen on the basis of assuming that in regions of branching (regions III and IV) the stimulated fibres may be thinner and thus characterized by higher '*A*' coefficients, while near the solitary tract, where the main axon usually passes, the '*A*' coefficients should be relatively low (Davies & Kubin, 1986). *C*, mean '*A*' coefficients ($\pm$S.D.) from the four regions of the NTS shown in *B*. Note that the mean values in all regions are higher than the steepness coefficient of the curve shown in *A* and that the curves were on the average steeper in the presumed regions of intense branching (regions III and IV).

with current ranges of 0–50 μA and 50–250 μA. It may also be noticed that a current of 250 μA would excite fibres characterized by '*A*' coefficients higher than 20000 μA mm^{-2} from a distance of about only 100 μm.

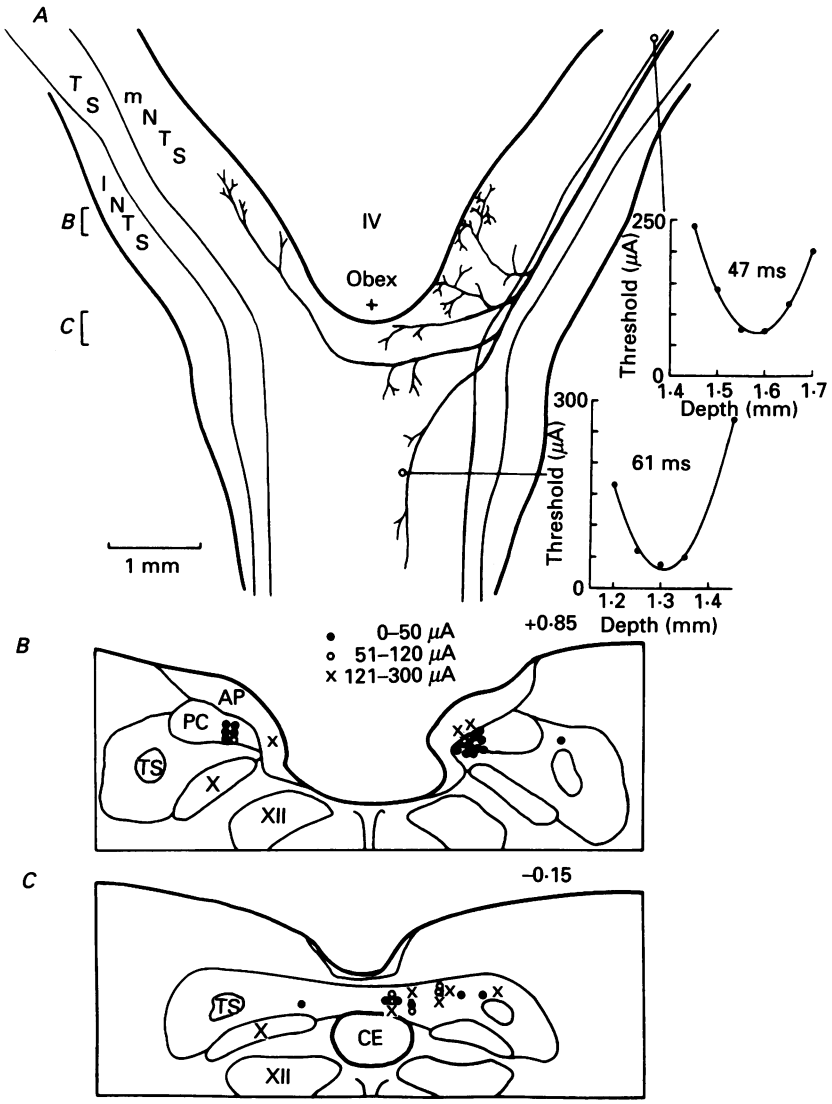

Fig. 6. Example of a branching pattern within the NTS of a bronchial C fibre. *A*, dorsal view of the NTS with the presumed course of the main axon and regions of branching shown semi-schematically; the number of short branches attached to a major collateral corresponds to the number of distant branches identified in that region. Two examples of depth–threshold curves are shown to the right. *B* and *C*, coronal sections through the dorsal medulla taken at levels marked by *B* and *C* in part *A*. The different symbols mark the locations of minimum threshold points for branches detected within 0·25 mm rostral or caudal to the planes shown. Note that rostral to the obex most branches were concentrated in the most medial portion of the NTS (*B*) while caudal to the obex most branches were found in the dorso-medial portion of the nucleus (*C*). Abbreviations: AP, area postrema; CE, central canal; PC, parvicellular portion of the NTS; TS, solitary tract; IV, fourth ventricle; X, dorsal motor nucleus of the vagus; XII, hypoglossal motor nucleus.

Localization and patterns of branching of bronchopulmonary C fibres within the NTS

As shown earlier in Fig. 3, we found evidence of branching only within a limited portion of the rostro-caudal extent of the NTS. Except for one bronchial receptor, substantial branching was found at levels extending from 1·8 mm rostral to 1·2 mm

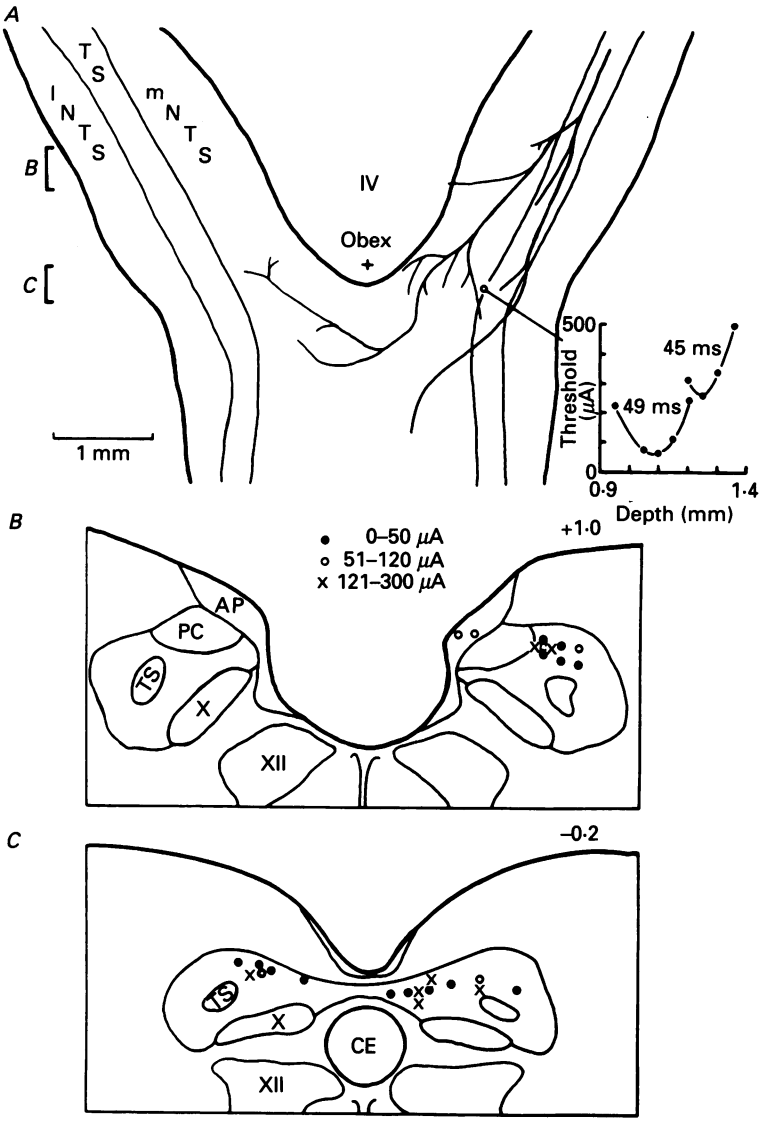

Fig. 7. Example of a branching pattern within the NTS of a pulmonary C fibre. *A*, dorsal view of the NTS as in Fig. 6*A*. The depth–threshold curves shown on the right indicate that two distinct branches were located in that particular penetration. *B* and *C*, coronal sections through the dorsal medulla. Other explanations and abbreviations as for Fig. 6.

caudal to the obex. (For one exceptional bronchial C fibre (cell 12 in Fig. 3), branches extended almost 3 mm caudal to the obex.) The contralateral branches found for some fibres, although less extensive, were located at similar rostro-caudal levels. Individual fibres classified as pulmonary tended to display a slightly more restricted distribution of branching regions in the rostro-caudal direction than bronchial fibres, but for the two subpopulations, the regions completely overlapped.

At levels 1–2 mm rostral to the obex, the main axons of the fibres were usually identified in the vicinity of the dorsal aspects of the solitary tract. It must be pointed out, however, that they were often located just dorsal or dorso-medial to the tract rather than within its main portion. This is in contrast to the pulmonary rapidly adapting receptors that have their axons within the solitary tract at levels rostral to the obex ipsilaterally (Davies & Kubin, 1986; Kalia & Richter, 1988).

The majority of low threshold points and branching sites was found concentrated in the most medial regions of the NTS. We found no branches lateral, ventro-lateral or ventral to the solitary tract, while a few branches were detected dorsal to the tract. For five fibres (two pulmonary and three bronchial), up to eleven (mean, 4) minimum threshold points were located within the area postrema. For two additional fibres such points were found just adjacent to the border between the NTS and area postrema.

In order to depict the relative density of branching in different regions for individual fibres, we have constructed semi-schematic maps that show, in a dorsal view of the NTS, the course of the main axon and its presumed ramifications as determined from the distance–latency and depth–threshold curve analyses (see the two preceding sections). Fine branches were attached to the presumed connecting branches so that their number corresponded to the number of responses with different latencies evoked from individual penetrations.

Figures 6 and 7 show two typical examples of such maps; one for a bronchial (Fig. 6) and one for a pulmonary (Fig. 7) fibre. The main axons of both fibres coursed parallel to the solitary tract. As shown in parts *B* and *C* of both figures, each fibre showed a rather restricted projection at levels rostral to the obex (within the medial NTS for the bronchial fibre and the dorsal NTS for the pulmonary fibre). Caudal to the obex, both fibres ramified widely within the dorsal portion of the nucleus. The pulmonary fibre shown in Fig. 8*A* was interesting in that all its branches were localized within or just adjacent to the ipsilateral area postrema rather than in the NTS; in fact, many of the lowest threshold points were found at depths less than 0·6 mm, indicating that the fibre projected to the area postrema (Fig. 8*B*).

Using the criteria of Loewy & Burton (1978), we have distinguished the following subnuclei within the caudal two thirds of the NTS: medial, intermediate, ventrolateral, lateral (subdivided by Kalia & Mesulam (1980*a*) into dorsal and dorsolateral subnuclei), parvicellular (gelatinosus, according to the nomenclature of Kalia & Mesulam, (1980*a*)), and commissural. No bronchopulmonary C fibre neurones sent branches to the intermediate and ventrolateral subnuclei. There were also very few branches found in the medial subnucleus immediately adjacent to the solitary tract. In contrast, the medial-most portion of the medial subnucleus contained an abundance of branches and the greatest density was found along the border between the medial and parvicellular subnuclei. Also, the parvicellular

subnucleus contained a substantial number of branches that, interestingly, were most concentrated along its border, while the centre contained only a few, mostly high threshold, points. Many branches were found in the medial portion of the lateral subnucleus (dorsal portion), and again the density was highest near its border with

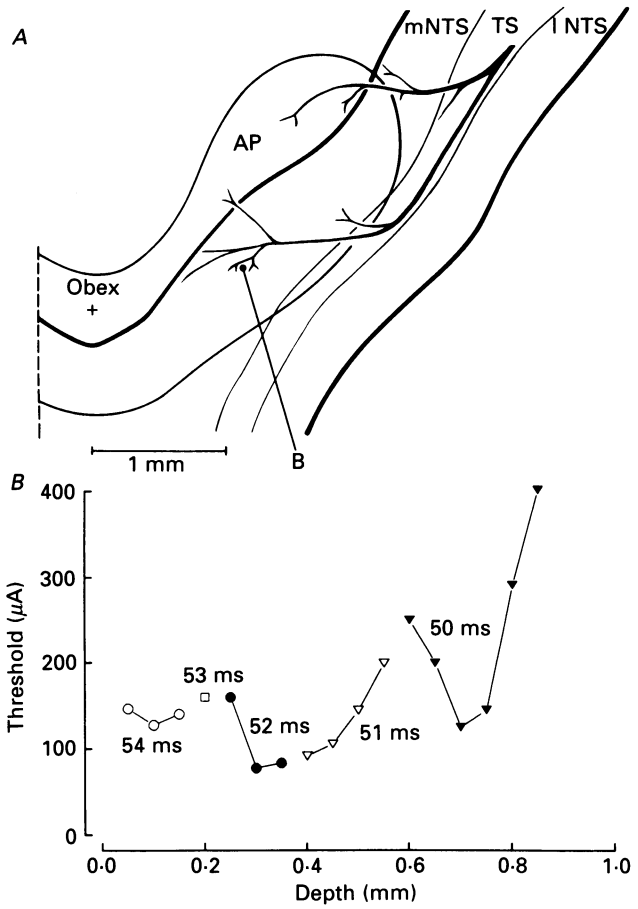

Fig. 8. Example of the central branching pattern of a pulmonary C fibre that projected only to the ipsilateral area postrema and vicinity. *A*, a dorsal view of the NTS and the area postrema (AP) ipsilateral to the cell body. *B*, depth–threshold curves obtained from a single penetration through the area postrema. Note that at least three distinct branches were stimulated, as judged by the three distinct minima on depth–threshold curves recorded as the stimulating electrode was moved in 50 μm steps from the surface to 0·8 mm below the surface.

the parvicellular subnucleus. There were, however, some branches in this region located far enough laterally from the parvicellular subnucleus to consider that the dorsal subnucleus itself was a target area. Finally, we found substantial branching in the dorsal portion of the commissural subnucleus. The branches in the contralateral NTS were distributed to the same subnuclei as ipsilaterally. The distributions of branches of pulmonary and bronchial fibres were similar.

Figure 9 shows the distribution of branches of all fibres studied superimposed on standard coronal cross-sections taken at 0·5 mm intervals through the caudal two-thirds of the NTS. Each symbol corresponds to the location of the lowest threshold site for one branch. Since we did not see any systematic differences in the regions of

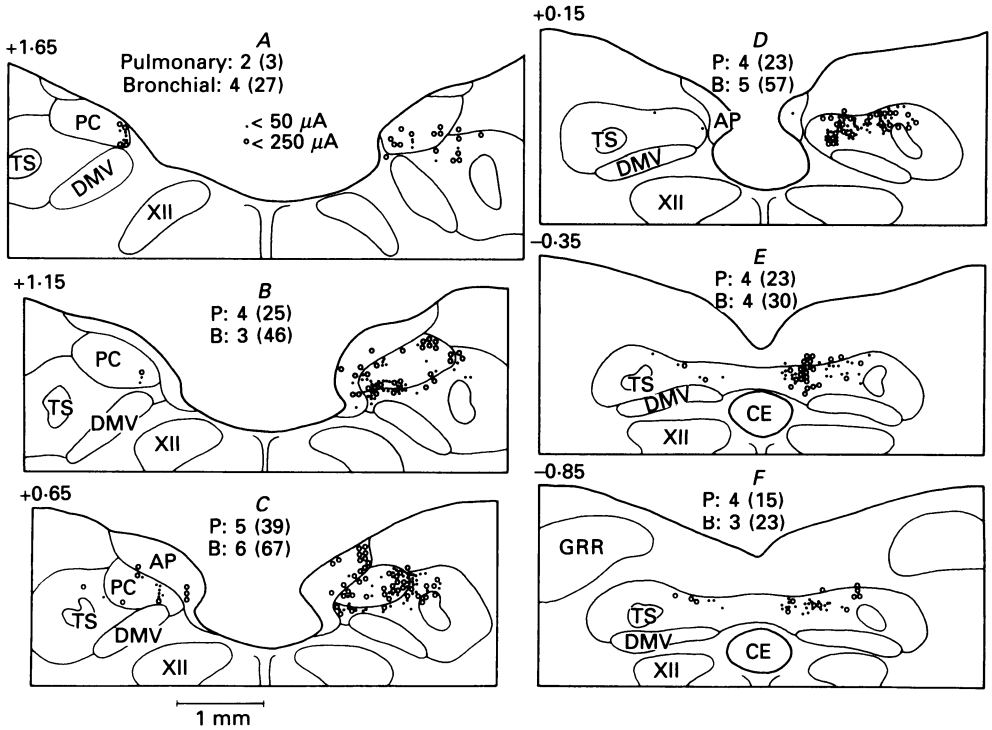

Fig. 9. Distribution of the minimum threshold points for each distinct central branch of all pulmonary and bronchial C fibres mapped. All sites with a minimum threshold of less than 50 μA (dots, ·) and less than 250 μA (circles, o), respectively, were plotted on standard coronal sections through the dorsal medulla taken at 0·5 mm intervals. The number of bronchial and pulmonary C fibre cells and the total number of branches that they contributed (in parentheses) are indicated above each cross-section. All points corresponding to the locations of the main axons, as well as those few branches of the three receptor cells that projected more caudal than 1·1 mm below the obex (cf. Fig. 3), have been omitted. Note that the minimum threshold points were consistently found around the parvicellular subnucleus rostral to the obex and within the dorsal part of the commissural subnucleus caudal to the obex. The average number of branches contributed by a single receptor cell type was consistently higher for bronchial than for pulmonary C fibres at each rostro-caudal level.

projection of bronchial and pulmonary fibres, we did not distinguish between branches belonging to the two receptor sub-types in this figure. We did indicate, however, how many fibres of each type contributed branches to each cross-section and the total number of branches contributed by each receptor subtype. The average density of branching was slightly higher for the bronchial than for the pulmonary fibres at all rostro-caudal levels. Different symbols were used to distinguish between

points at which the lowest threshold was less than 50 (dot) and 50–250 μA (circle), respectively. The low and high threshold points were intermixed in all regions except the area postrema, where we found very few low threshold points. That could be related to a relatively low density of branching and the particularly small diameter of fibres in that area, which reduced the chances of having the electrode placed close enough to a fibre to obtain a threshold lower than 50 μA. Points that most likely corresponded to the main axons of the cells were omitted in this figure, so that all the points may be regarded as reflecting the location of either terminal branches or intermediate branches that connected the terminals to the main axon. The parvicellular subnucleus was distinguished from the remaining portions of the NTS as it was our impression that the distribution of branches at levels rostral to the obex was related to the region of junction between this subnucleus and other structures (cf. Fig. 9*B* and *C*). At 0·15 mm rostral to the obex (Fig. 9*D*), where the parvicellular subnucleus was no longer distinguishable, the low threshold points were relatively widely scattered throughout the dorsomedial portion of the NTS, as if they were adjacent to the caudal end of the parvicellular subnucleus.

DISCUSSION

In this study, the third of a series in which we employed the technique of antidromic mapping to study the microcircuitry of vagal afferent pathways within the NTS (see Davies & Kubin, 1986; Davies, Kubin & Pack, 1987), we investigated the central distribution of pulmonary and bronchial C fibre afferents. Six pulmonary and six bronchial fibres were studied. They were identified on the basis of the latencies of their responses to capsaicin or phenyldiguanide injected into the pulmonary circulation. Pulmonary C fibres, in addition to showing a shorter response latency, responded with shorter bursts of action potentials having higher average firing rates than the bronchial C fibres (cf. Coleridge & Coleridge, 1984). The two subgroups also consistently differed in the conduction velocity of both the peripheral and central portions of their axons, with the bronchial fibre axons being slower conducting. These differences, although showing a statistical significance level of only 0·1, probably due to the small sample size, may contribute to the relative ease of detection and recording from pulmonary C fibres, when they are sampled from the vagal trunk. If that is the case, it is important to note that by recording from the receptor cell bodies in the nodose ganglion, we found the bronchial C fibres to be more numerous. This may be consistent with the results of Delpierre, Grimaud, Jammes & Mei (1981) who found equal numbers of bronchial and pulmonary C fibres in the nodose ganglion if one considers that these authors used a wider latency range to classify a cell as pulmonary.

Except for the fact that individual bronchial fibres seemed to have slightly more extensive projections within the NTS in the rostro-caudal direction and ramified more densely than the pulmonary fibres, the two C fibre types did not differ in the targets of their central projections. All projections were restricted to the medial regions of the NTS, the site where neurons excited by electrical stimulation of non-myelinated pulmonary vagal fibres were localized (Bennett, Goodchild, Kidd & McWilliam, 1985). At levels rostral to the obex, the distribution of the central

branches of all C fibres seemed to follow the outline of the parvicellular subnucleus of Loewy & Burton (1978). Low threshold points were found everywhere along the borders of this subnucleus, including the adjacent portions of the area postrema. The regions of the lateral and ventromedial edges of the parvicellular subnucleus contained particularly dense branching, with the majority of low threshold points located outside the boundaries of the subnucleus. Caudal to the obex, branches were observed throughout the dorsal aspects of the commissural subnucleus. The projection was bilateral with a strong ipsilateral predominance both rostral and caudal to the obex. Five fibres projected to ipsilateral NTS only.

The sites of bronchopulmonary C fibre projections determined in this study were contained within the anatomic regions of the projections of lung and airway receptors determined using the transganglionic transport of HRP by Kalia & Mesulam (1980*b*). The major difference between that and our study was that we found no projections of C fibres to the ventrolateral subnucleus and the region immediately medial and ventromedial to the solitary tract. This indicates that the heavy projection to those latter regions must have originated in lung and airway receptors of other modalities; pulmonary stretch receptors may have significantly contributed to those projections (Berger & Averill, 1983; Donoghue *et al.* 1982; Davies *et al.* 1987). Kalia & Mesulam (1980*b*) also described a substantial projection from the lungs and bronchi to the dorsolateral and interstitial subnuclei; the projections of our modality-identified fibres might slightly overlap with the medial region of the dorsolateral subnucleus, and we found no evidence of branching within the interstitial subnucleus. The latter finding may have some uncertainty owing to the small diameter of this subnucleus and its location adjacent to the solitary tract. Considering, however, that the main axons of C fibres were located in the dorsal portion or just above the tract, we feel that a substantial projection to the interstitial subnucleus, if present, would not have gone undetected with our technique. It is also noteworthy in this context that both the dorsolateral and interstitial subnuclei seem to be most heavily innervated by vagal afferents from the larynx (Nomura & Mizuno, 1983) and extrathoracic trachea (Kalia & Mesulam, 1980*b*) rather than by pulmonary or bronchial afferents. Similar to our study, Kalia & Mesulam (1980*b*) found the centre of the parvicellular subnucleus to be relatively devoid of afferents from the lungs or bronchi and to receive a substantial innervation from subdiaphragmatic vagal afferents.

Thus, our data show that bronchopulmonary C fibres project to a limited, clearly identified, portion of the NTS. These regions should now be investigated further as to their role in central processing of this afferent modality; perhaps, different portions of these regions will be found to subserve various aspects of respiratory, cardiovascular and somatic reflexes evoked by C fibre stimulation (Paintal, 1973; Coleridge & Coleridge, 1984). The fact that we did not find any differences in the NTS regions innervated by bronchial and pulmonary C fibres is consistent with a lack of qualitative differences between the reflex effects produced by the two receptor subtypes (Coleridge & Coleridge, 1984).

Bronchopulmonary C fibre receptors are powerfully excited by capsaicin and, as such, may be reasonably expected to contain substance P (SP) (Russell & Burchiel, 1984). Thus, it may be interesting to compare the distribution of SP and SP receptors

with the distribution of bronchopulmonary C fibre afferents within the NTS. Several studies have shown large amounts of SP (Maley & Elde, 1982; Baude, Lanoir, Vernier & Puizillout, 1989) and SP receptors (Maley, Sasek & Seybold, 1989) within the NTS of the cat. Interestingly, the areas labelled in all these studies include the regions of projections of C fibres as determined by us. Moreover, after a chronic unilateral vagotomy, there is a substantial drop in SP immunoreactivity in the dorsal part of the commissural subnucleus and in the region medial to the solitary tract at levels rostral to the obex (Baude *et al.* 1989). There is also a particularly good agreement between our results and the findings that the SP immunoreactivity (Maley & Elde, 1982) and SP receptors (Maley *et al.* 1989) are distributed along the borders of the parvicellular subnucleus. Thus, these data are compatible with the suggestion that SP is a transmitter for a large proportion of bronchopulmonary C fibres.

The present study and that of Donoghue *et al.* (1984) are the only ones so far that describe in some detail the central projections to the NTS of unmyelinated afferent fibres of identified modality. In both studies, the technique of antidromic mapping was employed as it currently seems to be the technique of choice to study non-myelinated fibres. The alternative technique, based on intra-axonal injection of tracers (primarily HRP) still poses substantial technical limitations when applied to very thin fibres (cf. Segiura, Lee & Perl, 1986) due to the difficulty of maintaining the penetration for a long enough time and the failure to transport adequate amounts of HRP into the very thin, preterminal branches of axons that densely ramify over a relatively wide area. Thus, for example, the density of HRP-visualized axonal branches of spinal interneurons that extensively ramified within the ventral horn decreased steeply over a distance of 600 μm; whereas, by using electrophysiological techniques, these axonal branches were shown to extend throughout several segments of the spinal cord (Bras, Cavallari, Jankowska & Kubin, 1989). Similarly, Kalia & Richter (1988), after injections of lectin labelled-HRP into the axons of pulmonary rapidly adapting receptor neurons placed rostral to the obex, found terminal branches within the dorsal, dorsolateral and intermediate subnuclei in agreement with our electrophysical mapping study (Davies & Kubin, 1986). However, they observed neither contralateral projections nor branches within the commissural subnucleus, whereas we found the ventral portion of the caudal NTS, bilaterally, to contain the highest density of thin branches. In contrast to the results with thin fibres, using HRP, the relatively thick axonal branches of spinal Ia afferents could be visualized over distances exceeding 6 mm (Ishizuka, Mannen, Hongo & Sasaki, 1979). Thus, it seems that, when applied to unmyelinated fibres, the antidromic mapping technique, although not capable of revealing local details of fibre morphology, may provide a more complete picture of the total projection areas than the technique of intra-axonal labelling. In addition, the antidromic technique is capable of providing an indirect evaluation of the relative thickness of axonal branches in different regions (Davies & Kubin, 1986), a feature that is not often appreciated and utilized to its full extent.

The present study provides new data to support the concept of a modality-specific (and thus functional) organization of the vagal primary afferent projections to the NTS. The projections of pulmonary stretch receptors (Donoghue *et al.* 1982; Berger & Averill, 1983; Davies *et al.* 1987; Kalia & Richter, 1985), rapidly adapting

receptors (Davies & Kubin, 1986; Kalia & Richter, 1988) and bronchopulmonary C fibres show little overlap. Within the commissural subnucleus, the branches of rapidly adapting receptors are concentrated along the ventral aspect (Kubin & Davies, 1986), while bronchopulmonary C fibres project dorsally. There are data pointing to some overlap in projections of afferents of different modalities within individual subnuclei or regions of the NTS, eg. arterial baro- and chemoreceptor afferent projections, as determined by transganglionic HRP transport (Claps & Torrealba, 1988; Torrealba & Claps, 1988) and by antidromic mapping (Donoghue *et al.* 1984) seem to heavily overlap with projections of pulmonary afferents. However, baroreceptor afferents, functionally identified and visualized with HRP, and their second order neurons were found in a caudal region of the NTS just dorsomedial to the solitary tract, an area not occupied by pulmonary afferents (Czachurski, Dembowsky, Seller, Nobiling & Taugner, 1988). Further, the cardiovascular response to pulmonary C fibre stimulation was not affected by laryngeal afferents, again pointing to a functional separation of the underlying central pathways (Daly & Kirkman, 1988). These examples point to a very fine functional organization of afferent pathways within the NTS and encourage further studies of local afferent and efferent connections of functionally identified subregions of the nucleus.

We are grateful to Dr Allan I. Pack for helpful discussions of the work and careful reading of the manuscript. We thank Ms Rosemarie Cohen for her excellent secretarial support. L. K. was on leave from the Department of Neurophysiology, Medical Research Centre, Polish Academy of Sciences, Warsaw, Poland. H. K. was on leave from the Department of Chest Medicine, School of Medicine, Chiba University, Japan. This study was supported by a grant from the National Heart, Lung and Blood Institute (HL-36621).

REFERENCES

AGOSTONI, E., CHINNOCK, J. E., DALY, M. DE B. & MURRAY, J. E. (1957). Functional and histological studies of the vagus nerve and its branches to the heart, lung and abdominal viscera in the cat. *Journal of Physiology* **135**, 182–205.

BAUDE, A., LANOIR, J., VERNIER, P. & PUIZILLOUT, J. J. (1989). Substance P-immunoreactivity in the dorsal medial region of the medulla in the cat: effects of nodosectomy. *Journal of Chemical Neuroanatomy* **2**, 67–81.

BENNETT, J. A., GOODCHILD, C. S., KIDD, C. & MCWILLIAM, P. N. (1985). Neurones in the brain stem of the cat excited by vagal afferent fibres from the heart and lungs. *Journal of Physiology* **369**, 1–15.

BERGER, A. J. & AVERILL, D. B. (1983). Projection of pulmonary stretch receptors to solitary tract region. *Journal of Neurophysiology* **49**, 819–830.

BRAS, H., CAVALLARI, P., JANKOWSKA, E. & KUBIN, L. (1989). Morphology of midlumbar interneurones relaying information from group II muscle afferents in the cat spinal cord. *Journal of Comparative Neurology* **290**, 1–15.

CLAPS, A. & TORREALBA, F. (1988). The carotid body connections: a WGA-HRP study in the cat. *Brain Research* **455**, 123–133.

COLERIDGE, J. C. G. & COLERIDGE, H. M. (1984). Afferent vagal C fibre innervation of the lungs and airways and its functional significance. *Reviews of Physiology, Biochemistry and Pharmacology* **99**, 1–110.

COTTLE, M. K. (1964). Degeneration studies of primary afferents of IXth and Xth cranial nerves in the cat. *Journal of Comparative Neurology* **122**, 329–345.

CZACHURSKI, J., DEMBOWSKY, K., SELLER, H., NOBILING, R. & TAUGNER, R. (1988). Morphology of electrophysiologically identified baroreceptor afferents and second order neurones in the brainstem of the cat. *Archives Italiennes de Biologie* **126**, 129–144.

DALY, M. DE B. & KIRKMAN, E. (1988). Cardiovascular responses to stimulation of pulmonary C fibres in the cat: their modulation by changes in respiration. *Journal of Physiology* **402**, 43–63.

DAVIES, R. O. & KUBIN, L. (1986). Projection of pulmonary rapidly adapting receptors to the medulla of the cat: an antidromic mapping study. *Journal of Physiology* **373**, 63–86.

DAVIES, R. O., KUBIN, L. & PACK, A. I. (1987). Pulmonary stretch receptor relay neurones of the cat: location and contralateral medullary projections. *Journal of Physiology* **383**, 571–585.

DELPIERRE, S., GRIMAUD, CH., JAMMES, Y. & MEI, N. (1981). Changes in activity of vagal bronchopulmonary C fibres by chemical and physical stimuli in the cat. *Journal of Physiology* **316**, 61–74.

DONOGHUE, S., FELDER, R. B., JORDAN, D. & SPYER, K. M. (1984). The central projections of carotid baroreceptors and chemoreceptors in the cat: a neurophysiological study. *Journal of Physiology* **347**, 397–409.

DONOGHUE, S., GARCIA, M., JORDAN, D. & SPYER, K. M. (1982). The brain-stem projections of pulmonary stretch afferent neurones in cats and rabbits. *Journal of Physiology* **322**, 353–363.

ISHIZUKA, N., MANNEN, H., HONGO, T. & SASAKI, S. (1979). Trajectory of group Ia afferent fibers stained with horseradish peroxidase in the lumbosacral spinal cord of the cat: three dimensional reconstruction from serial sections. *Journal of Comparative Neurology* **186**, 189–212.

JAMMES, Y., FORNARIS, E., MEI, N. & BARRAT, E. (1982). Afferent and efferent components of the bronchial vagal branches in cats. *Journal of the Autonomic Nervous System* **5**, 165–176.

KALIA, M. & MESULAM, M.-M. (1980*a*). Brain stem projections of sensory and motor components of the vagus complex in the cat. I. The cervical vagus and nodose ganglion. *Journal of Comparative Neurology* **193**, 435–465.

KALIA, M. & MESULAM, M.-M. (1980*b*). Brain stem projections of sensory and motor components of the vagus complex in the cat. II. Laryngeal, tracheobronchial, pulmonary, cardiac and gastrointestinal branches. *Journal of Comparative Neurology* **193**, 467–508.

KALIA, M. & RICHTER, D. (1985). Morphology of physiologically identified slowly adapting lung stretch receptor afferents stained with intra-axonal horseradish peroxidase in the nucleus of the tractus solitarius of the cat. I. A light microscopic analysis. *Journal of Comparative Neurology* **241**, 503–520.

KALIA, M. & RICHTER, D. (1988). Rapidly adapting pulmonary receptor afferents. I. Arborization in the nucleus of the tractus solitarius. *Journal of Comparative Neurology* **274**, 560–573.

KERR, F. W. L. (1962). Facial, vagal and glossopharyngeal nerves in the cat. *Archives of Neurology* **6**, 264–281.

KIRSTEN, E. B. & ST. JOHN, W. M. (1978). A feline decerebration technique with low mortality and long term homeostasis. *Journal of Pharmacological Methods* **1**, 263–268.

KUBIN, L. & DAVIES, R. O. (1987). Pulmonary C-fibers project to the caudal, medial nucleus tractus solitarius of the cat. *Federation Proceedings* **46**, 826.

KUBIN, L. & DAVIES, R. O. (1989). Distribution of broncho-pulmonary afferent C-fibers within the nucleus tractus solitarius (NTS) of the cat. *Proceedings of the International Union of Physiological Sciences* **XVII**, 74–75.

LIPSKI, J. (1981). Antidromic activation of neurones as an analytic tool in the study of the central nervous system. *Journal of Neuroscience Methods* **4**, 1–32.

LOEWY, A. D. & BURTON, H. (1978). Nuclei of the solitary tract: Efferent projections to the lower brain stem and spinal cord of the cat. *Journal of Comparative Neurology* **181**, 421–450.

MALEY, B. & ELDE, R. (1982). Immunohistochemical localization of putative neurotransmitters within the feline nucleus tractus solitarii. *Neuroscience* **7**, 2469–2490.

MALEY, B. E., SASEK, C. A. & SEYBOLD, V. S. (1989). Substance P binding sites in the nucleus tractus solitarius of the cat. *Peptides* **9**, 1301–1306.

MEI, N., CONDAMIN, M. & BOYER, A. (1980). The composition of the vagus nerve of the cat. *Cell and Tissue Research* **209**, 423–431.

NOMURA, S. & MIZUNO, N. (1983). Central distribution of efferent and afferent components of the cervical branches of the vagus nerve. *Anatomy and Embryology* **166**, 1–18.

PAINTAL, A. S. (1973). Vagal sensory receptors and their reflex effects. *Physiological Reviews* **53**, 159–227.

RUSSELL, L. C. & BURCHIEL, K. J. (1984). Neurophysiological effects of capsaicin. *Brain Research Reviews* **8**, 165–176.

SEGIURA, Y., LEE, C. L. & PERL, E. R. (1986). Central projections of identified, unmyelinated (C) afferent fibers innervating mammalian skin. *Science* **234**, 358–361.

TORREALBA, F. & CALDERÓN, F. (1990). Central projections of coarse and fine vagal axons of the cat. *Brain Research* **510**, 351–354.

TORREALBA, F. & CLAPS, A. (1988). The carotid sinus connections: a WGA-HRP study in the cat. *Brain Research* **455**, 134–143.